TOOL FLANK WEAR EFFECTS ON THE CUTTING EDGE SHRINK IN ULTRA-PRECISION RASTER FLY CUTTING

Guoqing Zhang[1], Suet To[2]
[1]Guangdong Provincial Key Laboratory of Micro/Nano Optomechatronics Engineering
Shenzhen University
Shenzhen, Guangdong, PR China
[2]State Key Laboratory of Ultra-precision Machining Technology
The Hong Kong Polytechnic University
Hong Kong, PR China

INSTRUCTIONS

In metal cutting, tool wear is an unavoidable phenomenon. There are many factors affecting the occurrence and characteristics of tool wear such as tool materials, cutting condition, tool geometry, and the workpiece materials being cut. In conventional cutting, the tool wear characteristics include: Nose wear, tool face wear, wear-land wear, cratering, and plastic flow [1]. However, the tool wear characteristics in ultra-precision machining are different from conventional machining. These differences include two aspects, first the cutting tool in ultra-precision machining is single crystal diamond, who owns super hardness and high thermal conductivity, which make the tool wear characteristic different [2]. Second, the diamond turnable workpiece material is broad, it not only include ductile materials like aluminum, copper, electroless nickel, but also include some brittle materials like ceramics, silicon, glass and so on [3-7]. Similar to conventional cutting, in ultra-precision cutting, tool wear occurs and features largely depend on the cutting condition, the workpiece material being cut. Cutting condition can seriously affect the tool life and tool wear characteristics. However, for diamond cutting ductile material such as copper and aluminum, a smooth and flat wear land is formed [8].

Ultra-precision raster fly cutting (UPRFC) is a typical intermittent cutting process whereby the diamond tool rotates across the spindle while the workpiece is fixed. The intermittent cutting property of UPRFC makes its tool wear characteristics different from other cutting process. This difference includes two aspects: one is that diamond tools are employed in the UPRFC cutting process, the extreme hardness and low friction coefficient of diamond tools delays the occurrence of tool wear [9]. The other one is that the discontinuous cutting mechanism of UPRFC reduces contact time between the diamond tool and workpiece, which allows for superior heat dispersion to suppress the occurrence of tool wear [10]. Until now, Yin et al. (2009) has conducted the research on tool wear characteristics in UPRFC, they identified the characteristics of diamond tool as fractures or micro chipping due to effects of impacts during the UPRFC process [11]. Our previous study found that the tool wear characteristics of UPRFC not only includes fractures of the cutting edge at the initial tool wear stage, but also includes material welding on the rake face, wear land and sub-wear-land formation at the steady wear stage, and micro-groove on the clearance of cutting tool [12]. Moreover, the tool wear characteristics identification methods and tool wear effects on the machined surface quality are investigated [13-15]. However, studies of tool flank wear effects on the cutting edge receding in UPRFC have not been conducted before.

In the present research, the tool flank wear characteristics are investigated, the effects of tool flank wear on cutting edge shrink is modeled, and cutting edge shrink effects on the surface roughness are discussed. The present research provides a deep insight into the relation between tool flank wear and cutting edge in ultra-precision machining.

EXPERIMENTS

In this study, a Precitech Freeform 705G (Precitech Inc., USA) five-axes CNC ultra-precision lath was used to perform the cutting experiment, which owns two typical cutting strategies: horizontal cutting and vertical cutting, as is shown in Fig. 1. In this study, a diamond tool designed and fabricated by Apex Inc., UK was chosen to cut the desired flat surface. Tool

geometry parameters are: tool nose radius of 0.631mm, rake angle of -2.5°, clearance angle of 15°. Cutting parameters used in this study are: feed rate: 200mm/min, depth of cut: 0.03mm, spindle speed: 4500rpm, swing distance: 28.35mm, step distance: 0.025mm. Cutting environment is lubricant on, cutting strategy is horizontal cutting. The workpiece material used in this experiment is brass. The total cutting distance is around 5000 meters.

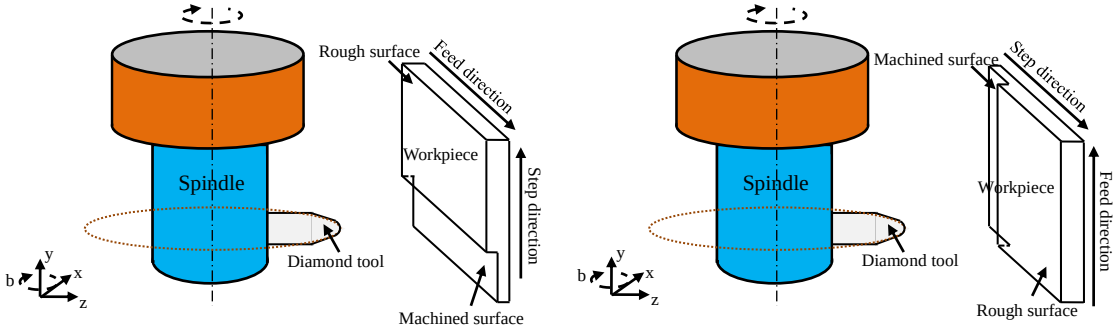

FIGURE 1. Cutting strategies in UPRFC

After cutting, the diamond tool was dismounted and inspected by Hitachi TM3000 scanning electron microscope (SEM), while the cutting edge profile was measured by a Park's XE-70 atomic force microscope (AFM).

RESULTS AND DISCUSSION

Tool Flank Wear Features

Diamond material has excellent mechanical properties such as extreme hardness and low friction coefficient. However, with the growing of the cutting distance, the mechanical wear of diamond tool is evitable. Fig.2 shows SEM tool wear figures after 5000m diamond flat cutting, it is found a smooth wear land is formed on the cutting edge. The wear land is wider at its central while thinner at its two sides, which is figured as crescent-like profile.

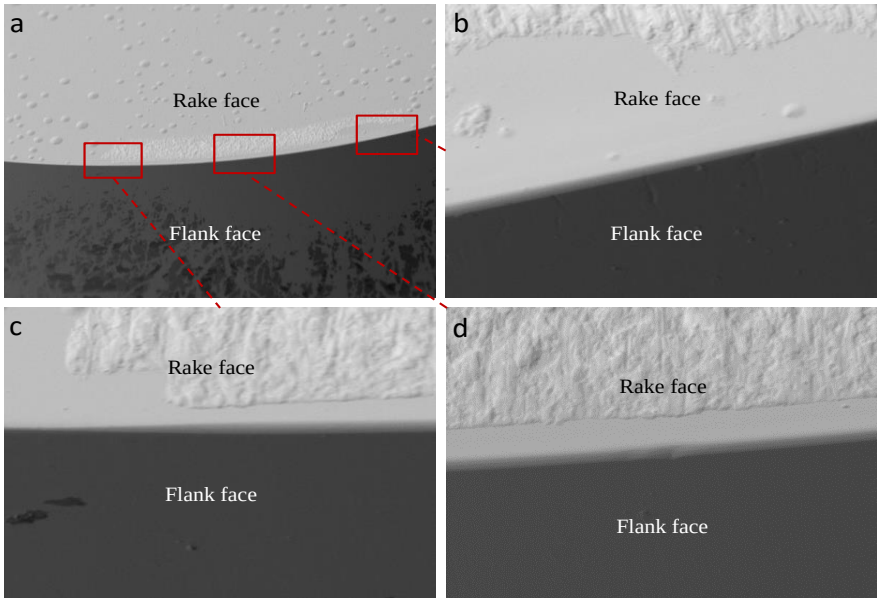

FIGURE 2. SEM figures of tool flank wear patterns after 5000m flat cutting

The occurrence of tool flank wear makes the cutting edge shrink and changes the tool geometry parameter. Therefore it will affect the form accuracy of machined surface.

Fig.3 shows the AFM figure of cutting edge, it is found that after a long distance cutting, a smooth wear land is formed on the cutting edge. The wear land has an angle ϕ with the rake face of diamond tool.

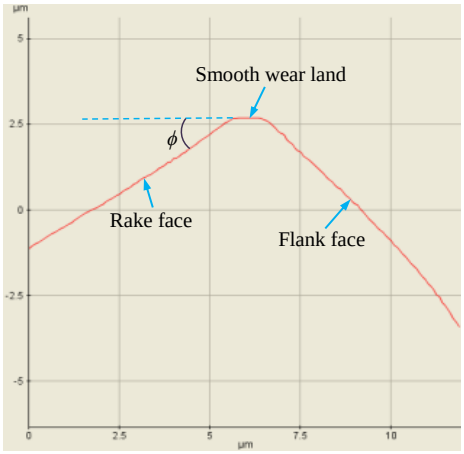

FIGURE 3. AFM photograph of cutting edge

Based on Fig.3, the width of wear land can be measured. Also the wear land angle can be measured.

Cutting Edge Shrinks Model

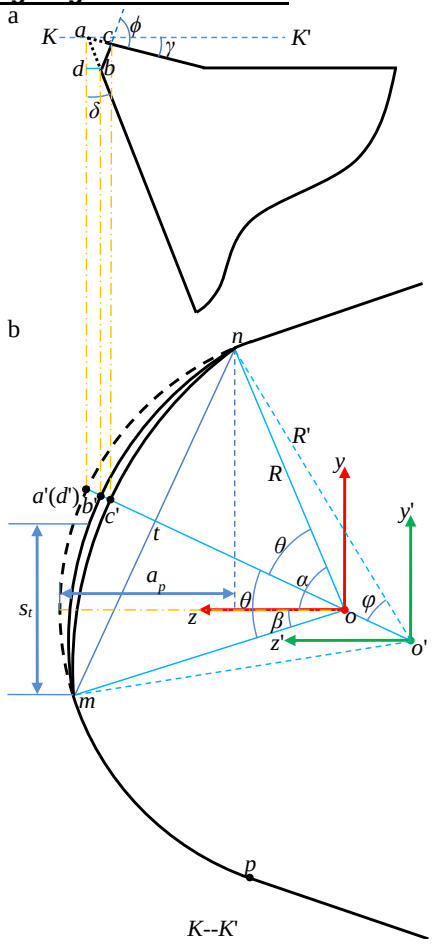

FIGURE 4. Schematic of the side view (a) and the top view(K--K' plane) (b) of tool flank wear

For clarity, two coordinate systems *o-yz* and *o'-y'z'* were established to present different arcs, as shown in Fig. 4 (b). In Fig. 4 (a), $|bc|$ is the wear land width, whose value can be identified from the cutting chips, and ϕ is the wear land angle, whose value is 40.5° since brass material being cut.

Based on the geometric relationship, the cutting edge retraction ($|bd|$) can be calculated from the Sine law. As is shown in Fig.4 (a), in triangle Δabc, $\angle acb = \phi$, $\angle bac = 90° - \delta - \gamma$, according to the Sine law:

$$\frac{|bc|}{\sin(90^\circ - \delta - \gamma)} = \frac{|ab|}{\sin\phi} \tag{1}$$

From Eq. (1), the length $|ab|$ can be calculated as:

$$|ab| = \frac{\sin\phi}{\sin(90^\circ - \delta - \gamma)}|bc| = \frac{\sin\phi}{\sin(90^\circ - \delta - \gamma)}w \tag{2}$$

Where w is the wear land width.

In triangle Δabd, the length $|bd|$ can be calculated as:

$$|bd| = |ab|\sin\delta = \frac{\sin\phi\sin\delta}{\sin(90^\circ - \delta - \gamma)}w \tag{3}$$

In the thrust plane *K-K'*, supposing $h_l = |b'd'|$, we obtain:

$$h_l = |b'd'| = |bd| = \frac{\sin\phi\sin\delta}{\sin(90^\circ - \delta - \gamma)}w \tag{4}$$

New Formed Tool Nose Radius

The tool flank wear in the UPRFC process makes the tool material loss-zone a crescent-like profile that is thicker at the center position while thinner at the two sides, as shown in Fig. 4 (b). Suppose the newly formed cutting edge and the original cutting edge are intersected at the point m and n, while the central point of new cutting edge arc mn is *b'*.

In Fig. 4 (b), according to the geometric relationship, we obtain:

$$\begin{cases} \cos\alpha = \left(R - a_p\right)/R \\ \sin\beta = \dfrac{s_t}{2R} \end{cases} \quad (5)$$

From Eq. (5), two angle α and β can be calculated as:

$$\begin{cases} \alpha = \arccos\left(\dfrac{R - a_p}{R}\right) \\ \beta = \arcsin\left(\dfrac{s_t}{2R}\right) \end{cases} \quad (6)$$

Therefore, θ in Fig. 4 (b) can be calculated as:

$$\theta = \frac{\alpha + \beta}{2} \quad (7)$$

In triangle ont in Fig. 4 (b), $|nt|$ can be solved as:

$$|nt| = R\sin\theta \quad (8)$$

Similarly, in triangle o'nt, $\sin\varphi$ is calculated as:

$$\sin\varphi = \frac{|nt|}{R'} = \frac{R\sin\theta}{R'} \quad (9)$$

From Eq. (9), the angle of φ can be computed as:

$$\varphi = \arcsin\left(\frac{R\sin\theta}{R'}\right) \quad (10)$$

Since the difference of $|d't|$ and $|b't|$ equals the height of the loss zone (hl), yields:

$$(R - R\cos\theta) - (R' - R'\cos\varphi) = h_l \quad (11)$$

Submitting Eq. (10) into φ in Eq. (11) yields:

$$R(1 - \cos\theta) - R'\left[1 - \cos\left(\arcsin\left(\frac{R\sin\theta}{R'}\right)\right)\right] = h_l \quad (12)$$

Eq. (12) can also be written as a function, as:

$$F(R') = R(1 - \cos\theta) - R'\left[1 - \cos\left(\arcsin\left(\frac{R\sin\theta}{R'}\right)\right)\right] - h_l = 0 \quad (13)$$

From Eq. (13), R' can be solved from numerical methods.

Effect Of Cutting Edge Shrink On The Machined Surface Roughness

Fig. 5 (a) shows that the surface topography is formed by the imprints of the cutting edge and that in the topography forming process, the intersection point of two original cutting edges is point *g*. However, the retraction of the cutting edge due to tool flank wear leads to the new intersection between the original cutting edge and worn cutting edge; the intersection point has been changed into point *u*, which causes a motion of the intersection point. In actuality, the retraction of cutting edge and the motion of intersection point are progressing simultaneously. Therefore, the retraction of cutting edge leads to the intersection of worn cutting edge at point *u*. Due to the bigger cutting edge radius of the worn cutting edge, the imprints of the worn cutting edge on the machined surface will cause a smaller surface roughness, as shown in Fig. 5 (b).

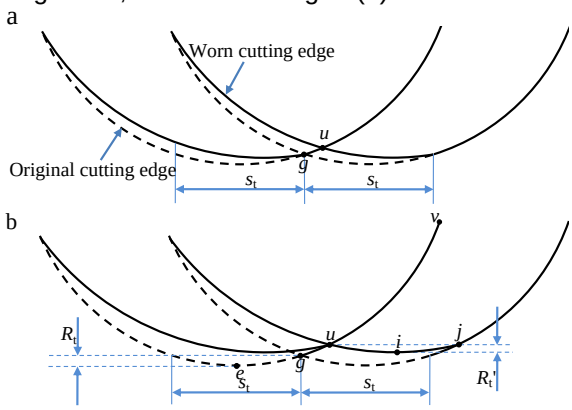

FIGURE 5. Tool flank wear effect on surface roughness

The theoretical peak-to-valley roughness in UPRFC is calculated as [14]:

$$\begin{cases} R_{t\_\min} = R_{t\_tool} = R - \sqrt{R^2 - (s_t/2)^2} \\ R_{t\_\max} = R_{t\_swing} + R_{t\_tool}/\cos\alpha = \\ s_w - \sqrt{s_w^2 - (f_e/2)^2} + \dfrac{s_w\left(R - \sqrt{R^2 - (s_t/2)^2}\right)}{\sqrt{s_w^2 - (f_e/2)^2}} \end{cases} \quad (14)$$

As the tool flank wear occurs, a new tool nose radius (R') is formed, the theoretical peak-to-valley roughness is changed into:

$$\begin{cases} R'_{t\_\min} = R' - \sqrt{R'^2 - (s_t/2)^2} \\ R'_{t\_\max} = s_w - \sqrt{s_w^2 - (f_e/2)^2} \\ + \dfrac{s_w\left(R' - \sqrt{R'^2 - (s_t/2)^2}\right)}{\sqrt{s_w^2 - (f_e/2)^2}} \end{cases} \quad (15)$$

CONCLUSIONS

In the present research, cutting edge shrink under tool flank wear and its effects on the machined surface roughness are investigated. Some specific conclusions drawn from the research are:

1. A smooth wear land is formed on the cutting edge as diamond cutting ductile materials, the smooth wear land has an angle with the rake face of diamond tools.

2. The occurrence of tool flank wear forms a new tool nose arc with a larger radius and a changed circle center.

3. The formation of tool flank wear affect the machined surface roughness, theoretically, cutting edge shrink reduce the surface roughness.

ACKNOWLEDGEMENTS

This project was supported by the National Natural Science Foundation of China (Grant No. 51505297 and 51675347) and the Natural Science Foundation of SZU (Grant No. 2016038).

REFERENCES

[1] Shaw Milton Clayton. Metal cutting principles. Vol. 2. Oxford university press. New York: 2005.

[2] Ding X, Liew WYH, Liu XD. Evaluation of machining performance of MMC with PCBN and PCD tools, Wear. 2005; 259(7):1225-1234.

[3] Rao B, Shin YC. Analysis on high-speed face-milling of 7075-T6 aluminum using carbide and diamond cutters. International Journal of Machine Tools and Manufacture. 2001; 41(12):1763-1781.

[4] Moriwaki T. Machinability of copper in ultra-precision micro diamond cutting. CIRP Annals-Manufacturing Technology. 1989; 38(1):115-118.

[5] Rahman KR, Rahman M, Neo KS, Sawa M, Maeda Y. Microgrooving on electroless nickel plated materials using a single crystal diamond tool. The International Journal of Advanced Manufacturing Technology. 2006; 27(9-10):911-917.

[6] Zeng WM, Li ZC, Pei ZJ, Treadwell C. Experimental observation of tool wear in rotary ultrasonic machining of advanced ceramics. International Journal of Machine Tools and Manufacture. 2005; 45(12): 1468-1473.

[7] Yan J, Zhang Z, Kuriyagawa T. Mechanism for material removal in diamond turning of reaction-bonded silicon carbide. International Journal of Machine Tools and Manufacture. 2009; 49(5):366-374.

[8] Wada R, Kodama H, Nakamura K, Mizutani Y, Shimura Y, Takenaka N. Wear characteristics of single crystal diamond tool. CIRP Annals-Manufacturing Technology. 1980; 29(1):47-52.

[9] Zuiker C, Krauss AR, Gruen DM. Physical and tribological properties of diamond films grown in argoncarbon plasmas. Thin Solid Films. 1995; 270(1):154-159.

[10] Song YC, Nezu K, Park CH, Moriwaki T. Tool wear control in single-crystal diamond cutting of steel by using the ultra-intermittent cutting method. International Journal of Machine Tools and Manufacture. 2009; 49(3–4):339-343.

[11] Yin ZQ, To S, Lee WB. Wear characteristics of diamond tool in ultra-precision raster milling. International Journal of Advanced Manufacturing Technology. 2009; 44(7-8):638-647.

[12] Zhang G, To S, Zhang S. Relationships of tool wear characteristics to cutting mechanics, chip formation, and surface quality in ultra-precision fly cutting. Int J Adv Manuf Technol. 2016; 83(1-4):133-144.

[13] Zhang G, To S, Xiao G. Novel tool wear monitoring method in ultra-precision raster milling using cutting chips. Precis Eng. 2014; 38(3):555–560.

[14] Zhang G, To S. A novel surface quality evaluation method in ultra-precision raster milling using cutting chips. J Mater Process Technol. 2015; 219:328–338.

[15] Zhang G, To S, Xiao G. The relation between chip morphology and tool wear in ultra-precision raster milling. Int J Mach Tools Manuf. 2014; 80-81:11-17.